RSC Advances

ROYAL SOCIETY OF CHEMISTRY

PAPER

View Article Online
View Journal | View Issue

Cite this: *RSC Adv.*, 2026, **16**, 20216

Tuning the hydrophobicity of glycine ester through *N*-acylation and introducing quaternary pyridinium groups enable the selectivity against Gram-positive bacteria

Aleena Pious,[a] Dharshini Karnan Singaravelu,[a] Srimari Srikanth,[a] Venkatasubramaian Ulaganathan,[a] Chithra Sivanandan,[b] Fadaa Alown,[c] Fuad Ameen[d] and Anbazhagan Veerappan *[a]

The membrane, which plays numerous fundamental biological roles, is a key target for drug discovery. To selectively gain access to the bacterial membrane, we synthesized a new series of 2-((*N*-(acylglycine ester) methyl)-1-methylpyridin-1-ium iodide) (QPyNAGe) compounds from glycine esters with tunable hydrophobicity by *N*-acylating them with fatty acids and introducing a cationic charge using quaternary pyridinium groups. The screening for antibacterial activity using the zone of inhibition method revealed that QPyNAGe is highly selective against Gram-positive bacteria. Among the compounds studied, 2-((*N*-(2-methoxy-2-oxoethyl)palmitamido)methyl)-1-methylpyridin-1-ium (QPyN16Ge) showed promising antibacterial activity (MIC, 3.91–7.81 μM), and 2-((*N*-(2-methoxy-2-oxoethyl)decanamido)methyl)-1-methylpyridin-1-ium (QPyN10Ge) had low antibacterial activity (MIC, 500–1000 μM) against the tested Gram-positive strains, including the methicillin-resistant *Staphylococcus aureus*. The hemocompatibility assay results showed that all QPyNAGe derivatives were more selective for bacteria than for human red blood cells. QPyN16Ge displayed the highest selectivity for bacteria, indicating that the hydrophobicity of the *N*-palmitoyl chain played a crucial role in enhancing its activity. QPyN16Ge exhibited rapid killing kinetics against planktonic MRSA compared with the standard antibiotic ciprofloxacin. The dipropylthiacarbocyanine iodide release experiment and the propidium iodide uptake assay demonstrated that QPyN16Ge depolarizes the cytoplasmic membrane more than QPyN10Ge and has greater membrane permeability. Scanning electron microscopy studies support the notion that QPyN16Ge damages the bacterial membranes, allowing their cellular contents to leak and inducing cell death. Resistance studies suggest that QPyN16Ge is less likely than ciprofloxacin to develop resistance against *S. aureus*. The therapeutic potential was demonstrated by rescuing MRSA-infected zebrafish with QPyN16Ge, reducing the bacterial burden in the animals.

Received 19th March 2026
Accepted 3rd April 2026

DOI: 10.1039/d6ra02317g

rsc.li/rsc-advances

1 Introduction

The emergence of superbugs and increasing evidence of microbial drug resistance have put the brakes on the golden era of antibiotics. A global survey has shown that about 1.2 million people died in 2019 from antibiotic-resistant bacterial infections. If unmanaged, resistant infections might kill 10 million people per year by 2050.[1] The World Health Organization has prioritized the development of antibacterial drugs to address drug resistance in *Mycobacterium tuberculosis*, *Salmonella*, *Shigella*, *Neisseria gonorrhoeae*, *Pseudomonas aeruginosa*, and *Staphylococcus aureus*. Recent years have seen an intensified research effort by several researchers, who have discovered diverse chemical structures for developing antimicrobial drugs.[2] In particular, many of these substances are structural mimics of microbial metabolic intermediates, also known as antimetabolites.[3] Consequently, natural or synthetic non-protein amino acids and their derivatives have emerged as an important class of drugs.[4] Similarly, single-chain amphiphilic lipids, such as fatty acids, have been recognized as broad-spectrum antibacterial agents.[5,6] Combining two physiologically relevant and biocompatible compounds to develop unique hybrid molecules is a popular method for synthesizing new

[a]*School of Chemical and Biotechnology, SASTRA Deemed University, Thanjavur, Tamil Nadu-613 401, India. E-mail: anbazhagan@scbt.sastra.edu; Fax: +91 4362-264120; Tel: +91 4362-264101-3689*

[b]*Department of Biotechnology of Medicines, Warsaw University of Technology, Warsaw, Poland*

[c]*Public Authority for Applied Education and Training (PAAET), Faculty of Basic Education/Science Department, Kuwait*

[d]*Department of Botany and Microbiology, College of Science, King Saud University, Riyadh, 11451, Saudi Arabia*

bioactives. In this regard, lipoamino acid (LAA) derivatives have been shown to inhibit lipase and exhibit anti-inflammatory, antibacterial, and antifungal properties.[7–9] The lipophilicity of LAA is expected to provide membrane-mimicking properties that may aid drug delivery by facilitating the passage through biomembranes. However, the non-specific nature of LAA can cause hemolysis, and its low solubility limits its therapeutic potential. Therefore, it is imperative to develop new antimicrobials with high solubility and specificity for bacteria rather than their host cells. Considering that bacterial membranes have a negative surface charge, positively charged organic counterions can be used instead of conventional sodium and potassium salts to form cationic systems that are more soluble in water and exhibit strong antibacterial activity.[10] Quaternary ammonium salts (QAs) are recognized for their antimicrobial properties and are utilized as disinfectants and antiseptics.[11] Despite their advantages, QAs negatively impact the environment and human health. Prolonged exposure to QAs affects the immune system, reproductive system, and endocrine function.[12] Strong sorption of QAs onto solids and organic particles restricts their biodegradation, prolongs their environmental persistence, and causes toxicity.[13] Therefore, it is crucial to create new QAs that are biocompatible, efficient against microorganisms, and easily degradable in the environment. We recently reported the antibacterial, antifungal, and antibiofilm activities of the pyridinium salts of *N*-acyl ethanolamine (cNAE).[14,15] cNAEs kill bacteria by damaging their membranes, disrupting biofilm formation, and exhibiting lower toxicity towards human red blood cells. A review of the literature revealed that *N*-acyl amino acids have been utilized as biostatic additives, enzyme inhibitors, antiproliferative agents, antifungals, and other therapeutic agents.[16] Ricinoleic acid-based LAA displays good antibacterial and antibiofilm activity against Gram-positive bacteria.[17]

Glycine is categorized as a non-essential amino acid but is indispensable for the synthesis of peptides and proteins, for the production of creatine, glutathione, porphyrins, and purines, and for the conjugation of bile acids and xenobiotics.[18] At higher concentrations, glycine inhibits bacterial growth and is used as an antibacterial agent in food due to its low toxicity to animals.[19] *N*-acylglycines, such as *N*-arachidonoyl glycine and *N*-palmitoylglycine, act as signalling molecules with roles in antinociception, anti-inflammation, and cell proliferation.[20] Considering the benefits of LAA, herein, we aimed to synthesize an antimicrobial from *N*-acylglycine ester and add cationic functionality by conjugating with a 2-methylene-1-methylpyridinium iodide group. A facile method was developed to synthesize 2-((*N*-(acylglycine ester)methyl)-1-methylpyridin-1-ium iodide) (QPyNAGe), and the molecular hydrophobicity was modulated by varying the length of the *N*-acyl chain. Antimicrobial testing revealed that QPyNAGe exhibits *N*-acyl chain length-dependent antibacterial activity, with specificity for Gram-positive bacteria. To understand the mechanism of action, the effects of QPyNAGe on bacterial membranes were investigated. The biocompatibility of QPyNAGe was assessed using a hemolytic assay, and the results are discussed.

2 Materials and methods

The SI contains a detailed presentation of the materials and processes. The techniques employed in this paper are briefly described below.

2.1 Materials

Pyridine-2-carboxaldehyde and thionyl chloride were purchased from Hyma, India. Fatty acids and glycine methyl ester were purchased from TCI, India. Triethylamine and sodium cyanoborohydride were purchased from SRL Chemicals. Methyl iodide was purchased from LOBA Chemie. The media and reagents for microbiology were obtained from HiMedia, India.

2.2 Synthesis of *N*-acyl-*N*-(pyridin-2-ylmethyl)glycine methyl ester (PyNAGe)

The *N*-acyl-*N*-(pyridin-2-ylmethyl)glycine methyl ester was synthesized from glycine. The reaction progress was monitored by thin-layer chromatography. The reaction mass was extracted using ethyl acetate and a saturated solution of NH_4Cl. The crude product of methyl 2-((pyridin-2-ylmethyl)amino)acetate obtained from the organic layer was subjected to *N*-acylation without further purification. After the reaction was complete, the crude mass was extracted with ethyl acetate and saturated with $NaHCO_3$. The organic layer was dried and purified by column chromatography (mesh size, 60–120). The product was eluted with ethyl acetate : hexane (30 : 70); the reaction yield was approximately 75%. The product was confirmed by ^1H and ^{13}C NMR spectroscopy (see SI).

2.3 Synthesis of 2-((*N*-(acylglycine ester)methyl)-1-methylpyridin-1-ium iodide (QPyNAGe)

PyNAGe was quaternized using methyl iodide. Following the completion of the reaction, the solvent and excess methyl iodide were removed using a rotary evaporator. The obtained precipitate was washed several times with acetone and hexane to obtain the pure product. The reaction yield was approximately 95%. The purity of the product was confirmed by ^1H NMR and ^{13}C NMR spectroscopy and HRMS (see SI).

2.4 Antimicrobial activity

The antimicrobial activity of the synthesized molecules was assessed by the zone of inhibition (ZOI) assay.[21] The strains used in this study are *Staphylococcus aureus* (MTCC3160), methicillin-susceptible *Staphylococcus aureus* (ATCC29213), methicillin-resistant *Staphylococcus aureus* (ATCC43300), *Enterococcus faecalis* (ATCC29212), *Streptococcus iniae* (ATCC29178), *Escherichia coli* (MTCC723), uropathogenic *Escherichia coli* (MTCC729), *Pseudomonas aeruginosa* (MTCC1688), carbapenem-resistant *Acinetobacter baumannii* (MTCC12889), and *Proteus mirabilis* (MTCC425). The formation of a zone around the well indicates antimicrobial activity.

2.5 Determination of minimum inhibitory concentration and minimum bactericidal concentration

The minimum inhibitory concentration (MIC) of all QPyNAGe derivatives was determined using turbidometry and resazurin microtiter assay (REMA) in accordance with CLSI broth microdilution guidelines.[22] The minimum bactericidal concentration (MBC) was determined by swabbing 10 μL of treated cells from the MIC plate onto an agar plate after the turbidity measurements. The experiments were repeated three times to test the reproducibility.

2.6 Time-kill kinetics

The killing efficiency of QPyNAGe was investigated using the time-kill kinetics method.[23] The reference antibiotic, ciprofloxacin (CIP), was used as a positive control, and bacteria that were not treated with QPyN16Ge served as a negative control. Three separate experiments were conducted in triplicate, and the log CFU mL^{-1} was plotted *versus* time.

2.7 Hemocompatibility assay

The hemolytic concentration (HLC) is determined by tracking cell lysis and heme release.[24] All experiments were conducted in accordance with the guidelines of the Indian Council of Medical Research (ICMR) and were approved by the ethics committee at SASTRA University.

2.8 Membrane permeability assay

Bacterial cells were treated with 1X MIC QPyNAGe for 2 h at 37 °C, then collected by centrifugation at 3000 rpm. The treated cells were exposed to 50 μM propidium iodide (PI), and fluorescence was measured at 617 nm with excitation at 535 nm. Untreated cells and cells treated with 1 mM Triton X-100 were used as the negative control and positive control, respectively. The percentage of membrane permeability was calculated using eqn (1) as follows:[25]

$$\%\ \text{Membrane permeability} = [(F_s - F_n)/(F_p - F_n)] \times 100, \quad (1)$$

where F_n is the initial PI fluorescence from the untreated cells, and F_s and F_p are the PI fluorescence from the cells treated with QPyNAGe and Triton X-100, respectively.

2.9 Cytoplasmic membrane depolarization assay

The cytoplasmic membrane depolarization was analysed using membrane potential-sensitive fluorescent dye 3,3′-dipropylthiacarbocyanine iodide (DiSC3(5)). Briefly, 500 μL of dye-loaded cells were treated with 1X MIC QPyNAGe for 10 min. After treatment, the fluorescence emission was recorded at 670 nm by exciting at 622 nm. Untreated cells and cells treated with 2 mM Triton X-100 were used as negative and positive controls, respectively. The percentage of membrane depolarization was calculated using eqn (1).

2.10 Reactive oxygen species assay

Typically, cells were treated after exposure to 10 μM 2′-7′-dichlorodihydrofluorescein diacetate (DCFH-DA) and incubated at 37 °C for 30 min. After incubation, fluorescence emission was observed at 525 nm (excitation wavelength: 485 nm). The negative and positive controls were untreated cells and cells treated with 10 μL of 30% hydrogen peroxide.[26]

2.11 Resistant testing

The ability of bacteria to develop resistance to QPyNAGe was assessed by determining MIC after repeated exposure to the drug.[27] Ciprofloxacin (Cip) was used as the standard antibiotic control. The experiment was repeated 29 times with repeated exposure at 0.5X MIC. The increase in the MIC indicates the development of resistance.

2.12 Animal testing

The therapeutic efficacy of QPyNAGe was evaluated using a zebrafish animal model, following the procedure described in ref. 28. The experiments were approved by the Institutional Ethics Committee (CPCSEA-493/SASTRA/IAEC/RPP) of SASTRA University, India, and conducted in accordance with the guidelines for laboratory animal facilities set by CPCSEA (Central Act 26 of 1982). For the experiments, twenty healthy fish were infected intramuscularly with 10 μL of 1.0×10^8 CFU mL^{-1} MRSA and allowed 3 h to spread the infection. After treatment, fish from both groups were collected at defined time intervals and sacrificed, and their muscle tissue was dissected from the opposite side of the bacterial injection. About 30 mg of the muscle tissue was homogenized, diluted appropriately, and plated on a nutrient agar plate. The plates were incubated at 37 °C for 12 h, and the colonies were counted and reported as CFU mL^{-1}.

3 Results and discussion

3.1 Design and synthesis of 2-(*N*-acylglycine ester)-1-methylpyridin-1-ium iodide

Esters are the most commonly employed functional groups in the prodrug design due to their chemical stability, ease of synthesis, and efficient release of the active drug *via* enzymatic hydrolysis by ubiquitous esterases in the body.[29] Having learned about the glycine antimicrobial activity at high doses, we developed pyridine-conjugated glycine ester (methyl 2-((pyridin-2-ylmethyl)amino)acetate) and added fatty acids through *N*-acylation to obtain *N*-acyl-*N*-(pyridin-2-ylmethyl)glycine ester (PyNAGe) [Scheme 1]. Fatty acids are known to have antibacterial properties, and their lipophilicity enables molecules to enter cells. The molecular hydrophobicity can be modulated by utilizing fatty acids with varying acyl chain lengths. To target the negatively charged surface charge of bacterial membranes, the pyridine group was quaternized with methyl iodide to obtain 2-(*N*-acylglycine ester)-1-methylpyridin-1-ium iodide (QPyNAGe). The obtained products were confirmed by ^1H NMR and ^{13}C NMR spectroscopy and HRMS [see SI Fig. S1–S25].

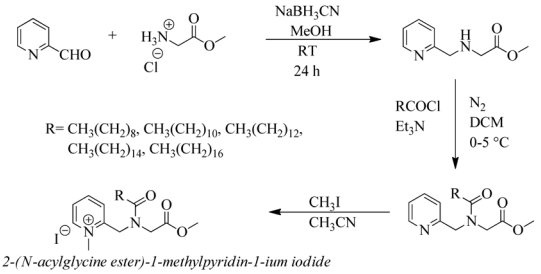

Scheme 1 Synthesis of 2-(*N*-acylglycine ester)-1-methylpyridin-1-ium iodide (QPyNAGe).

Representative discussions on the structural elucidation, based on ^{1}H NMR, ^{13}C NMR, and HRMS analyses, are presented in the SI.

3.2 Antimicrobial activity

The antibacterial activity of QPyNAGe against Gram-positive and Gram-negative bacterial strains was assessed by the zone of inhibition (ZOI) experiment. ZOI testing enables a quick and qualitative assessment of drug efficacy in inhibiting bacterial growth.[30] Before quaternization, there was no ZOI activity detected for PyNAGe. Interestingly, the QPyNAGe demonstrated a ZOI against the tested Gram-positive bacteria, indicating that quaternization is essential for recognizing the negative bacterial surface. In contrast, QPyNAGe had no activity against Gram-negative bacteria [see SI Fig. S26], implying that QPyNAGe is specific against Gram-positive bacteria. After observing poor sensitivity to Gram-negative bacteria, we focused our study on Gram-positive bacteria, including drug-sensitive strains, such as *S. aureus*, methicillin-sensitive *S. aureus*, *Enterococcus faecalis*, and *Streptococcus iniae*, as well as drug-resistant strains such as methicillin-resistant *S. aureus*. Table 1 shows the QPyNAGe MIC values against Gram-positive bacteria. As shown in Table 1, the MICs differ among the QPyNAGe derivatives, indicating that increasing the methylene groups in the *N*-acyl chain significantly affects the MIC. The higher MICs observed with QPyN10Ge and QPyN12Ge suggest reduced antibacterial activity, attributed to the *N*-acyl chain's insufficient hydrophobicity, which impedes membrane penetration in bacteria. Interestingly, QPyN14Ge, QPyN16Ge, and QPyN18Ge had lower MICs, with QPyN16Ge having the lowest MIC of the tested strains. The results indicate that molecular hydrophobicity is a key component in the antibacterial activity of the QPyNAGe class of molecules. The antibacterial activity observed with QPyNAGe suggests that *N*-acylation contributes to more than just anchoring within the bacterial membrane; it may also directly influence the bacterial membrane's network. Further assessment of these findings requires in-depth metabolomics research.

Table 1 MICs determined using REMA analysis

	MIC (μM)				
Molecule	*S. aureus*	MSSA	MRSA[a]	*S. iniae*	*E. faecalis*
QPyN10Ge	500	500	1000	1000	1000
QPyN12Ge	62.5	31.25	125	250	125
QPyN14Ge	3.91	3.91	15.63	31.25	7.81
QPyN16Ge	3.91	3.91	7.81	7.81	7.81
QPyN18Ge	3.91	7.81	7.81	7.81	15.63

[a] drug-resistant.

3.3 Bactericidal activity

To evaluate if QPyNAGe possesses bactericidal, bacteriostatic, or both properties, aliquots from wells with MICs of 0X, 0.5X, 1X, 2X, 4X, and 8X were spotted on appropriate agar plates. The concentration that did not result in bacterial colony formation was noted as the minimum bactericidal concentration (MBC). The experiment was shown to be correctly carried out by comparing the MBC data with that of the control well (untreated), which displayed bacterial growth [see SI Fig. S27]. The MBC values are presented in Table S1 (see SI Table S1). It was demonstrated that QPyN16Ge and QPyN18Ge are highly effective and exhibit bactericidal activity at 1X MIC, suggesting that the *N*-acyl chain provides an adequate hydrophilic-lipophilic balance that permits QPyN16Ge and QPyN18Ge to permeate the cell wall and kill the cells. Following the observation of bactericidal activity, we examined the killing rate to assess the effectiveness of QPyN16Ge against MRSA. The untreated cells exhibited exponential growth as expected (Fig. 1). As noted from Fig. 1, the QPyN16Ge treatment significantly reduced CFU within 30 minutes at 1X MIC. However, ciprofloxacin, a standard antibiotic, took one hour to induce a response, as evidenced by decreased CFU, and achieved lower CFU levels after two hours. Strikingly, the reduced CFU observed with ciprofloxacin treatment after two hours was

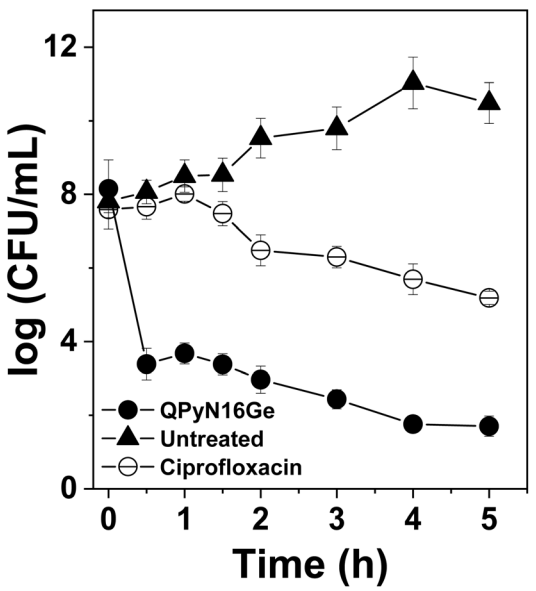

Fig. 1 Time-kill kinetics assay showing the efficacy of QPyN16Ge in killing MRSA. The experiments were performed in triplicate ($n = 3$), and the results are presented as mean ± SD.

higher compared to QPyN16Me treatment, suggesting that QPyN16Ge kills bacteria more quickly and effectively than ciprofloxacin.

3.4 Hemocompatibility

Any new antimicrobial drugs disclosed must include information regarding their toxicity to mammalian cells. To investigate the toxicity of QPyNAGe, we conducted a hemolytic assay using human red blood cells (RBC), and the results were reported as the ratio of the hemolytic concentration to the MBC (Table S2). The hemolytic concentrations (HLC) of QPyN10Ge, QPyN12Ge, QPyN14Ge, QPyN16Ge, and QPyNAGe were 4000, 1000, 500, 500, and 500 μM, respectively. The toxicity towards RBCs was found to increase with the hydrophobicity of the *N*-acyl chain. Nevertheless, the HLC/MBC ratio for QPyNAGe was higher than the MIC, indicating that the molecules were effective against pathogenic microbes while being safe to mammalian cell lines. When analyzing the HLC and MBC ratios, we found that QPyN10Ge and QPyN12Ge had lower values, indicating toxicity to RBC, whereas QPyN14Ge had somewhat higher values, indicating mild toxicity. Interestingly, QPyN16Ge and QPyN18Ge showed higher HLC/MBC values, indicating that these drugs are more selective for bacteria than mammalian cells. The findings suggest that HLB plays a crucial role in determining the selectivity of drugs between the host and bacterium.

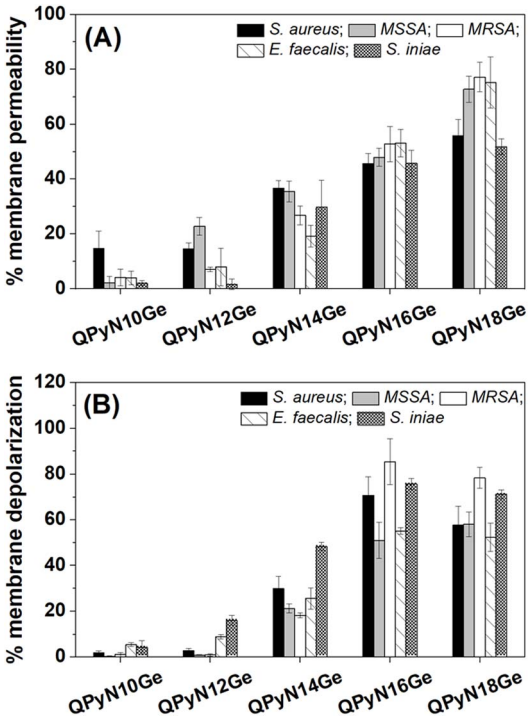

Fig. 2 Membrane-active mechanism of action: (A) membrane permeability and (B) cytoplasmic membrane depolarization measured after the treatment with QPyNAGe at a concentration of 7.81 μM.

3.5 Effect of hydrophobicity in the membrane–active mode of action

The membrane–active properties of QPyNAGe were determined by measuring the membrane permeabilization and cytoplasmic membrane depolarization against *S. aureus*, MSSA, *E. faecalis*, *S. iniae*, and MRSA. It is known that increasing the number of methylene groups in an acyl chain of a hydrocarbon increases the hydrophobicity. To assess the influence of QPyNAGe hydrophobicity on permeability and bacterial cell wall disruption, the propidium iodide (PI) uptake assay was used. PI is membrane-impermeable, but useful in assessing membrane disruption in cells by measuring its non-specific interaction with DNA, which results in enhanced fluorescence. The study used a fixed concentration of 7.81 μM to compare the membrane–active properties of the reported QPyNAGe (Fig. 2). Untreated cells and cells treated with the membrane-permeabilizing agent TritonX-100 were used as negative and positive controls, respectively. As shown in Fig. 2A, the membrane-permeabilizing activity of QPyNAGe increases with increasing chain length, regardless of the bacteria tested. The data suggest that QPyN18Ge has the highest permeability, indicating that the long acyl chain causes extensive membrane damage and efficiently kills the bacteria. Notably, different bacteria showed differential membrane-permeabilizing activity for the same molecules, which could be attributed to the differential membrane compositions.

To determine whether QPyNAGe kills bacteria by disrupting the electrical potential across the bacterial cytoplasmic membrane, we analysed the membrane potential using the fluorescent dye 3,3′-dipropylthiadicarbocyanine iodide (DiSC3(5)). The fluorescence intensity increased after treatment, compared with untreated cells, indicating a change in the membrane potential. Notably, bacteria treated with QPyN18Ge showed a higher percentage of membrane depolarization than those treated with other QPyNAGe, indicating that the hydrophobicity of the molecules played a significant role in disrupting the membrane potential (Fig. 2B). These findings suggest that the hydrophobicity of the acyl chain is crucial for interacting with the bacterial membrane. A scanning electron microscopy (SEM) study provided additional evidence of membrane damage (Fig. 3). The SEM image of untreated cells exhibited normal morphology, characterized by a smooth surface and intact cell membranes (Fig. 3A). As illustrated in Fig. 3B, treatment with QPyN18Ge resulted in shrunken, crumpled, and fractured cells. The loss of cell membrane integrity causes intracellular substances to leak out, leading to cell death in MRSA.

Bactericidal antibiotics, such as quinolones, aminoglycosides, and β-lactams, cause oxidative stress by producing excessive reactive oxygen species (ROS) to kill bacteria. Thus, the ability of QPyNAGe to produce ROS was investigated using the dichlorofluorescein (DCF) assay. The experiment involves cells taking up DCFH-DA and undergoing deacetylation by esterase to produce a non-fluorescent compound, which ROS subsequently oxidize to produce the fluorescent molecule DCF. The untreated cells (negative control) exposed to DCFH-DA showed weak fluorescence, suggesting that the cells are healthy and that the ROS production is balanced by the natural

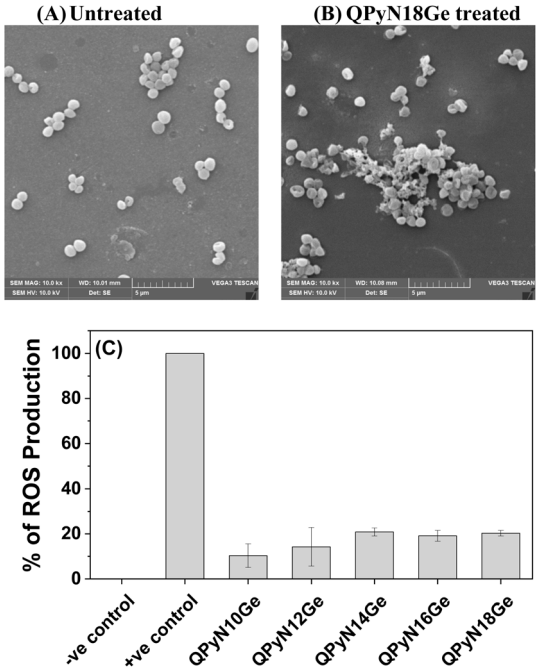

Fig. 3 Scanning electron microscopy images of MRSA: (A) untreated and (B) treated with 7.8 μM of QPyN18Ge. (C) ROS assay of MRSA treated with 7.8 μM of QPyN18Ge and stained with DCFH-DA. The experiments were performed in triplicate, and the mean ± SD is presented.

antioxidant defense mechanism (Fig. 3C). Fig. 3C shows that the cells treated with endogenous ROS, such as hydrogen peroxide (positive control), uptake DCFH-DA and show strong fluorescence, indicating that H_2O_2 induces oxidative stress due to redox imbalance. Interestingly, cells treated with QPyNAGe showed a lower ROS level than the positive control, suggesting that ROS may not be the primary mechanism of membrane disruption. Excessive ROS production by bactericidal antibiotics can induce mitochondrial dysfunction and oxidative damage in host cells, leading to antibiotic-related toxicity. The findings support that QPyNAGe is a safer choice as a novel antibacterial agent against drug-resistant bacteria, as it damages membranes without producing excessive ROS.

3.6 Resistance study

Microorganisms are evolving to resist traditional drugs that target a single system or pathway. For example, ciprofloxacin (CIP) targets specific enzymes, such as DNA gyrase and topoisomerase IV, leading to the emergence of quinolone-resistant *S. aureus*. Thus, we evaluated *S. aureus* ability to develop resistance to QPyNAGe. In line with expectations, *S. aureus* began to develop resistance to CIP after 10 passages, which increased during the subsequent passages, and its MIC increased to 256-fold at 29 passages. In contrast, *S. aureus* has a limited ability to build resistance against QPyN16Ge; even after 29 passes, the MIC increased just fourfold (Fig. 4). The findings confirm the hypothesis that QPyNAGe membrane–disruption activity and multiple targeting potential provide benefits for developing this series of compounds into resistance-proof antimicrobial drugs.

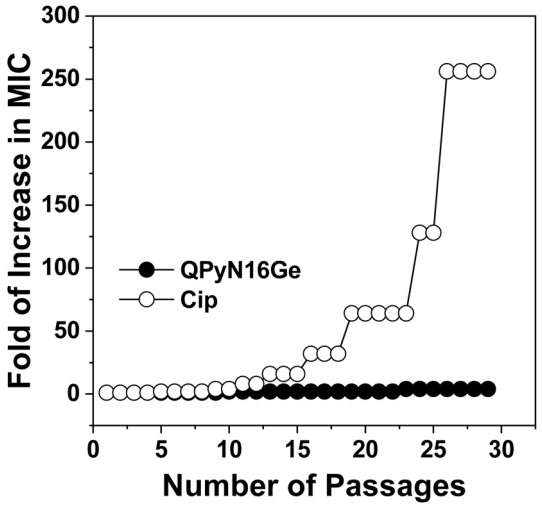

Fig. 4 Plot of the resistance of *S. aureus* to QPyN16Ge and the antibiotic ciprofloxacin.

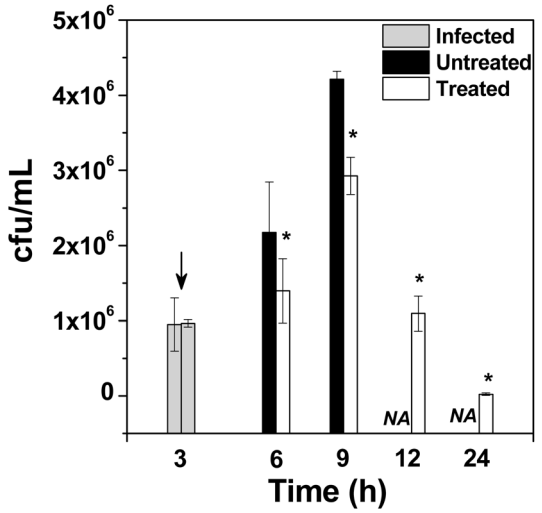

Fig. 5 Bacterial load in the muscle of infected and treated zebrafish. The fish were infected with MRSA and treated with 7.8 μM of QPyN16Ge. The arrow indicates the time point at which the treatment started. NA means no fish are alive at that time point. Error bars indicate SD. * denotes a statistically significant difference ($p < 0.05$) calculated through one-way ANOVA.

3.7 *In vivo* antibacterial activity

Zebrafish were chosen as an animal model for drug testing because 84% of human disease-related genes have orthologs in the zebrafish genome.[31] In this study, zebrafish were infected intramuscularly by injecting MRSA, and an attempt was made to rescue them from the infection using QPyN16Ge treatment. The fish that had contracted the infection slowed down after 6 h and succumbed to it within 14 h. In contrast, fish treated with QPyN16Ge quickly recovered from the infection and resumed

their normal lifestyles. After observing the survival of fish following QPyN16Ge treatment, we measured the bacterial load in tissues before and after treatment. During the first three hours of infection, the fish muscle had a large number of bacteria, as evidenced by a higher CFU mL^{-1} (Fig. 5). The bacterial burden in the muscles of the untreated fish increased over time. In contrast, fish treated with QPyN16Ge after the three-hour infection period showed a significant reduction in CFU (Fig. 5). These findings indicate that QPyN16Ge inhibited the spread of infection, enabling the fish to recover. Overall, the study demonstrated the potential of QPyN16Ge in treating drug-resistant infections and elucidated its *in vitro* antibacterial mechanism. Further studies in cell lines and higher animal models, such as rodents, could enable us to recommend these molecules for the next phase of testing.

4 Conclusion

A series of pyridinium-based *N*-acylglycine esters was developed by varying the acyl chain length, thereby modulating molecular hydrophobicity and enabling them to permeate bacterial membranes. The antibacterial assay revealed that the QPyNAGe series has selective activity against Gram-positive bacteria. Antibacterial and hemocompatibility studies indicated that the molecule containing the *N*-palmitoyl chain showed promising activity and was selective for killing bacteria over mammalian cells. Mechanistic studies showed that QPyN16Ge kills bacteria by efficiently penetrating their membranes, depolarizing the cytoplasmic membrane, disrupting membrane packing, and inducing cell leakage. In addition to membrane damage, the possibility of interfering with cell wall biosynthesis was assessed by molecular docking and molecular dynamics simulation. This suggested that QPyN16Ge may interact with the cell wall biosynthesis enzyme FemA, and this interaction may influence cell wall formation (see SI, Fig. S28 and Table S2). QPyN16Ge kills MRSA more effectively than ciprofloxacin, and the bacteria are unable to develop resistance to this compound even after 29 consecutive passages. The results demonstrate that an optimal hydrophilic-lipophilic balance is crucial for developing nontoxic, membrane-active compounds with potent antibacterial activity. More importantly, QPyN16Ge demonstrated *in vivo* activity by drastically reducing the bacterial burden and rescuing MRSA-infected zebrafish. Additional studies using mammalian cell lines and higher animals, such as rodents, may reveal the feasibility of employing the QPyNAGe class of compounds to treat drug-resistant Gram-positive bacterial infections.

Ethical statement

All experiments were conducted in accordance with the guidelines of the Indian Council of Medical Research (ICMR) and were approved by the ethics committee at the SASTRA University. Informed consents were obtained from the human participants of this study.

The experiments were approved by the Institutional Ethics Committee (CPCSEA-493/SASTRA/IAEC/RPP) of the SASTRA University, India, and conducted in accordance with the guidelines for laboratory animal facilities set by the CPCSEA (Central Act 26 of 1982).

Conflicts of interest

There are no conflicts to declare.

Data availability

All data collected were presented in the main text as diagram and supporting information (SI). All raw data will be available upon request. Supplementary information: detail methods, NMR, HRMS, MBC plates, molecular docking and molecular dynamics simulations. See DOI: https://doi.org/10.1039/d6ra02317g.

Acknowledgements

V. A. acknowledges the Indian Council of Medical Research, Government of India (67/7/2022-DDI/BMS) and TRR grant (SASTRA-TRR-SCBT-1-25112024), for financial support. A. P. and D. K. S. thank the SASTRA Deemed University for the teaching assistantships. FA acknowledges the funding from the ongoing research funding program (ORF-2026-364) at the King Saud University, Riyadh, Saudi Arabia. SS acknowledges the UGC, India, for awarding the Savitribai Jyotirao Phule SRF for Single Girl Child (UGCES-22-OB-TAM-F-SJSGC-4474).

References

1 K. W. K. Tang, B. C. Millar and J. E. Moore, Antimicrobial Resistance (AMR), *Br J Biomed Sci*, 2023, **80**, 11387, DOI: 10.3389/bjbs.2023.11387.
2 V. H. Krishnaprasad, V. Nayak and S. Kumar, World Health Organisation's Bacterial Pathogen Priority List (BPPL) 2017 and BPPL 2024 to combat global antimicrobial resistance crisis:'challenges and opportunities, *J. Antimicrob. Chemother.*, 2025, **80**, 2061–2069, DOI: 10.1093/jac/dkaf167.
3 M. S. Butler, W. Vollmer, E. C. A. Goodall, *et al.*, A Review of Antibacterial Candidates with New Modes of Action, *ACS Infect Dis*, 2024, **10**, 3440–3474, DOI: 10.1021/acsinfecdis.4c00218.
4 M. G. Nowak, A. S. Skwarecki and M. J. Milewska, Amino Acid Based Antimicrobial Agents-Synthesis and Properties, *ChemMedChem*, 2021, **16**, 3513–3544, DOI: 10.1002/cmdc.202100503.
5 H. Arellano, V. Nardello-Rataj, S. Szunerits, *et al.*, Saturated long chain fatty acids as possible natural alternative antibacterial agents: Opportunities and challenges, *Adv. Colloid Interface Sci.*, 2023, **318**, 102952, DOI: 10.1016/j.cis.2023.102952.
6 G. Casillas-Vargas, C. Ocasio-Malavé, S. Medina, *et al.*, Antibacterial fatty acids: An update of possible mechanisms of action and implications in the development of the next-generation of antibacterial agents,

Prog. Lipid Res., 2021, **82**, 101093, DOI: 10.1016/j.plipres.2021.101093.

7 T. Tsujita, M. Sumiyoshi, T. Takaku, *et al.*, Inhibition of lipases by ε-polylysine, *J. Lipid Res.*, 2003, **44**, 2278–2286, DOI: 10.1194/jlr.M300151-JLR200.

8 S. S. Kaki, S. Arukali, P. V. Korlipara, *et al.*, Synthesis and biological evaluation of novel lipoamino acid derivatives, *Bioorg. Med. Chem. Lett.*, 2016, **26**, 209–212, DOI: 10.1016/j.bmcl.2015.10.086.

9 R. Takenouchi, K. Inoue, Y. Kambe, *et al.*, N-arachidonoyl glycine induces macrophage apoptosis via GPR18, *Biochem. Biophys. Res. Commun.*, 2012, **418**, 366–371, DOI: 10.1016/j.bbrc.2012.01.027.

10 G. C. Lainioti and D. Druvari, Designing Antibacterial-Based Quaternary Ammonium Coatings (Surfaces) or Films for Biomedical Applications: Recent Advances, *Int. J. Mol. Sci.*, 2024, **25**, 12264, DOI: 10.3390/ijms252212264.

11 Z. Zhou, S. Zhou, X. Zhang, *et al.*, Quaternary Ammonium Salts: Insights into Synthesis and New Directions in Antibacterial Applications, *Bioconjug Chem*, 2023, **34**, 302–325, DOI: 10.1021/acs.bioconjchem.2c00598.

12 W. A. Arnold, A. Blum, J. Branyan, *et al.*, Quaternary Ammonium Compounds: A Chemical Class of Emerging Concern, *Environ. Sci. Technol.*, 2023, **57**, 7645–7665, DOI: 10.1021/acs.est.2c08244.

13 D. S. Villarreal-Lucio, R. Flores-Ramírez, J. M. Izar-Landeta, L. A. Bernal-Jácome and K. X. Vargas-Berrones, Impacts associated with the excessive use of quaternary ammonium salts in disinfectants and a perspective for their substitution, *J. Water Process Eng.*, 2025, **77**, 108607, DOI: 10.1016/j.jwpe.2025.108607.

14 S. Bala Subramaniyan, D. Karnan Singaravelu, T. Raman, *et al.*, Antimicrobial lipids loaded on lectin display reduced MIC, curtail pathogenesis and protect zebrafish from reinfection by immunomodulation, *Microb. Pathog.*, 2024, **193**, 106744, DOI: 10.1016/j.micpath.2024.106744.

15 S. Bala Subramaniyan, S. Ramesh, S. Rajendran, *et al.*, Dual Function Antimicrobial Loaded Lectin Carrier: A Strategy to Overcome Biomolecular Interference without Detectable Resistance, *Bioconjug. Chem.*, 2021, **32**, 1823–1833, DOI: 10.1021/acs.bioconjchem.1c00281.

16 S. Arul Prakash and R. K. Kamlekar, Function and therapeutic potential of N-acyl amino acids, *Chem. Phys. Lipids*, 2021, **239**, 105114, DOI: 10.1016/j.chemphyslip.2021.105114.

17 Y. Mohini, R. B. Prasad, M. S. Karuna, *et al.*, Synthesis and biological evaluation of ricinoleic acid-based lipoamino acid derivatives, *Bioorg. Med. Chem. Lett.*, 2016, **26**, 5198–5202, DOI: 10.1016/j.bmcl.2016.09.063.

18 M. Holeček, Glycine as a conditionally essential amino acid and its relationship to l-serine, *Metabolism*, 2025, **170**, 156330, DOI: 10.1016/j.metabol.2025.156330.

19 C. Giordano and S. Barnini, Glycine restores the sensitivity to antibiotics in multidrug-resistant bacteria, *Microbiol. Spectr.*, 2024, **12**, e0016424, DOI: 10.1128/spectrum.00164-24.

20 J. R. Foster, S. Ueno, M. X. Chen, *et al.*, N-Palmitoylglycine and other N-acylamides activate the lipid receptor G2A/GPR132, *Pharmacol Res Perspect*, 2019, **7**, e00542, DOI: 10.1002/prp2.542.

21 T. J. Hossain, Methods for screening and evaluation of antimicrobial activity: A review of protocols, advantages, and limitations, *Eur J Microbiol Immunol*, 2024, **14**, 97–115, DOI: 10.1556/1886.2024.00035.

22 M. D. Rakhmawatie, T. Wibawa, P. Lisdiyanti, *et al.*, Evaluation of crystal violet decolorization assay and resazurin microplate assay for antimycobacterial screening, *Heliyon*, 2019, **5**, e02263, DOI: 10.1016/j.heliyon.2019.e02263.

23 N. Nordholt, L.-Y. Sobisch, A. Gödt, *et al.*, Heterogeneous survival upon disinfection underlies evolution of increased tolerance, *Microbiol. Spectr.*, 2024, **12**, e0327622, DOI: 10.1128/spectrum.03276-22.

24 E. Bondi, N. Bloise, M. Soccio, *et al.*, Synthesis of Flexible Random Copolymers of Poly(butylene trans-1,4-ciclohexanedicarboxylate) Containing Pripol Moiety as Potential Candidates for Vascular Applications: Solid-State Characterization and Preliminary In Vitro Biocompatibility and Hemocompatibility, *Biomacromolecules*, 2025, **26**, 2882–2899, DOI: 10.1021/acs.biomac.4c01668.

25 D. K. Singaravelu, D. N. Binjawhar, F. Ameen, *et al.*, Lectin-Fortified Cationic Copper Sulfide Nanoparticles Gain Dual Targeting Capabilities to Treat Carbapenem-Resistant Acinetobacter baumannii Infection, *ACS Omega*, 2022, **7**, 43934–43944, DOI: 10.1021/acsomega.2c05252.

26 A. Pious, R. Sabarinath, D. Karnan Singaravelu, *et al.*, Amphiphilic cationic 2-morpholinoethanol analogues synthesis and study of N-alkylation role in self-assembly and anticandida activity, *Colloids Surf. B Biointerfaces*, 2025, **255**, 114892, DOI: 10.1016/j.colsurfb.2025.114892.

27 T. Maeda and C. Furusawa, Laboratory Evolution of Antimicrobial Resistance in Bacteria to Develop Rational Treatment Strategies, *Antibiotics*, 2024, **13**, 94, DOI: 10.3390/antibiotics13010094.

28 S. B. Subramaniyan, S. Vijayakumar, S. Megarajan, *et al.*, Remarkable Effect of Jacalin in Diminishing the Protein Corona Interference in the Antibacterial Activity of Pectin-Capped Copper Sulfide Nanoparticles, *ACS Omega*, 2019, **4**, 14049–14056, DOI: 10.1021/acsomega.9b01886.

29 E. M. Larsen and R. J. Johnson, Microbial esterases and ester prodrugs: An unlikely marriage for combating antibiotic resistance, *Drug Dev. Res.*, 2019, **80**, 33–47, DOI: 10.1002/ddr.21468.

30 N. Kadeřábková, A. J. S. Mahmood and D. A. I. Mavridou, Antibiotic susceptibility testing using minimum inhibitory concentration (MIC) assays, *NPJ Antimicrob Resist.*, 2024, **2**, 37, DOI: 10.1038/s44259-024-00051-6.

31 M. Adhish and I. Manjubala, Effectiveness of zebrafish models in understanding human diseases-A review of models, *Heliyon*, 2023, **9**, e14557, DOI: 10.1016/j.heliyon.2023.e14557.